

Polyether Based Thermoplastic Polyurethane Melt Blown Nonwovens

Terezie Zapletalova¹, Stephen Michielsen², Behnam Pourdeyhimi²

¹Freudenberg Nonwovens (North America), PO Box 15910, Durham, North Carolina 27704

USA ²North Carolina State University, 2401 Research Dr., Raleigh, North Carolina 27695-8301 USA

Correspondence to:

Stephen Michielsen, Ph.D., email: Stephen_michielsen@ncsu.edu

Abstract

A series of melt blown samples were produced from three hardness grades of ether based thermoplastic polyurethane elastomers (TPU). The fabrics were tested to investigate their structure-property relationship in a melt blown process. Solution viscosities of the web were only 20-26% of there original values indicating a large loss in polymer molecular weight during melt blowing. Fiber diameter distributions measured on melt blown samples were found comparable to those made with more conventional polymers. The fiber orientation distribution functions (ODF) suggest slight fiber orientation in machine direction. Tensile and elongation properties depended on die-to-collector distance (DCD), polymer hardness and fiber ODF. A strong relationship between the tensile strength and die-to-collector distance was identified and attributed to reduced interfiber adhesion in the web with increasing DCD. The reduction in adhesion was attributed to greater extents of solidification before reaching the forming belt for longer DCDs. This paper is the first in a series relating the influence of the melt blowing process parameters on the polymer properties and the nonwoven fabric properties for block thermoplastic elastomers.

Introduction

Since the introduction of thermoplastic elastomers into the market, there has been a great effort to use these materials in nonwoven fabrics. Except for patent literature, nonwoven materials made with thermoplastic elastomer polymers have rarely been reported. Thermoplastic elastomer melt blown webs have been used as a single layer, intimately blended with other types of fiber or laminated into composites [1-11]. Commercial use of melt blown elastomeric webs has been reported predominantly by 3M and Kimberly-Clark [12, 13].

Thermoplastic elastomers are copolymeric materials made from hard and soft polymeric chain components. Typically, hard and soft segment species are not miscible in each other, which leads to a phase separated structure. Bonart [16] states that crosslinking in thermoplastic elastomers is mostly brought about by the secondary valence interactions within the hard segment domains. Even though it is expected that the hard segment regions would be crystalline, their ability to crystallize appears to be inhibited and the regions are regarded as paracrystalline [17]. The degree of crystallinity in hard segment domains can be increased by annealing [18] as well as a combination of stretching and annealing [19].

Thermoplastic polyurethanes (TPUs) are one class of thermoplastic elastomers (TPE). They can be processed from the molten state using conventional thermoplastic processing technologies while recovering their rubber-like properties upon solidification. TPUs contain polymer hard segment regions, which create anchor points having the same function as crosslinks in vulcanized rubbers. The morphology of MDI-BDO-based hard segments in stretched and annealed polyurethane films was extensively studied by Blackwell et al [19-22]. When compared with other chain extender types, poly(MDI-BDO) was found to create the most crystalline segment [23,24]. In these studies a typical annealing cycle consisted of exposing the sample to relatively high temperature for long times such as 130°C for 7 days [18], which is not practical in nonwoven fabric production.

Due to their arrangement as a phase-separated system, each component contained in a thermoplastic elastomer maintains most of its properties, such as melting point or glass transition temperature. Mechanical properties of thermoplastic elastomers depend greatly on the ratio of hard and soft segments, as well as length of each species within the polymer chain. Thermoplastic elastomeric polymers tend to exhibit lower melting points and are more pliable as the soft segment content is increased. The upper practical limit to soft segment content is ~90%. With the increase of soft segment phase in polymer composition, the recovery properties start to deteriorate and the polymer becomes “sticky”. With higher content of the hard phase, the polymer hardness and the glass transition temperature increases. At 60-70 wt % of hard segment, the material behaves more like a plastic than an elastomer. Thus the hard/soft segment ratio is closely linked to polymer durometer hardness [25].

The melt blowing process was first introduced by Wentz [26] as a means to create a collection medium for radioactive particles in the upper atmosphere. The melt blown nonwoven process is a unique technology in which molten polymer emerging from a series of small orifices on the die is subjected to two hot, high-velocity air streams that cause attenuation and fibrillation of the polymer into very fine fibers. The fibers made in this process are typically 1-20 microns in diameter. Owing to their small fiber diameter and high surface area, melt blown substrates are typically used as barrier layers and filters. During melt blowing, the fibers are deposited on a moving collector belt, usually creating a layer of self-bonded fibers. The basis weight of a melt blown fibrous layer can be varied by adjusting the speed of the collector belt. A typical structure of a melt blown nonwoven can be seen in *Figure 1*. The melt blown process requires polymeric melts to be of a very low viscosity, which is usually achieved by using a polymer with a high melt-flow rate (low molecular weight) and by adjusting the melt temperature during processing.

Once the fiber breaks loose from the molten polymer pool at the die tip, it is propelled downward to the collector belt. The die-to-collector distance (DCD) and the air jet velocity determine the amount of time a newly created fiber spends suspended in air before it is forced into contact with the rest of the fibrous substrate during the collection process. The melt temperature, air velocity,

air temperature, and DCD have major influences on how much solidification and crystallization occurs before the fiber comes into contact with other fibers already on the collector belt.

The objective of this paper is to determine the relationship between processing conditions and fabric performance properties of melt blown nonwoven fabrics made with three different hardness grades of a polyether-based thermoplastic polyurethane with hard segment chemistry based on 4,4'-diphenylmethane diisocyanate (MDI) and 1,4-butanediol (BDO). This paper is the first in a series relating the influence of the melt blowing process parameters on the polymer properties to the nonwoven fabric properties.

Experimental

Melt Blown Fabric Production: Three polyether polyurethanes with MDI-BDO-based hard segments were provided by BASF in hardness grades of 80A, 90A and 98A durometer hardness. This spans the useful range of thermoplastic elastomers made with MDI-BDO hard segment and polyether-based soft segment. Softer grades are too sticky, while harder grades have poor elastomeric properties. A series of melt blown fabrics was produced on the Nonwoven Cooperative Research Center's (NCRC) melt blowing line. Processing temperatures were adjusted for each polymer grade to maintain die pressures in the range 3.1-3.8 MPa (450-550 psi) and polymer flow rates of 0.5 grams per hole per minute. The process air temperature was maintained at the same temperature as the die temperature, the hot air flow and the quench air were set at 70% and 20% of fan capacity respectively. For a few samples, the polymer pressures at the die fell outside the desired range. The die temperatures used during melt blowing are listed in *Table I*. Melt blown fabrics were produced at three DCD levels – 14, 20 and 30.5 cm (5.5 in, 8.0 in and 12.0 in) with basis weights of 50 g/m² and 100 g/m².

Differential Scanning Calorimetry (DSC): Heating scans were run from -50°C to 250°C at 20°C/min. Endothermic ranges and peak temperatures are shown in *Table I*.

Fiber Diameter Distribution: Scanning Electron Microscopy (SEM) images were obtained for each fabric and 150 diameter measurements were obtained using NCRC Image Analysis software [27].

Fiber Orientation Distribution Function (ODF): Five transmitted light optical microscopy images were obtained for each sample and analyzed by NCRC Image Analysis software. Cosine squared anisotropy ratio was then computed as [28]:

$$H_t = 2 \langle \cos^2 \phi \rangle - 1 \quad (3)$$

where ϕ is the angle between the cross direction of the nonwoven and the fiber axis. The average value of $\cos^2 \phi$ is

$$\langle \cos^2 \phi \rangle = \int_{-\pi/2}^{\pi/2} f_i(\phi) \cos^2(\phi) d\phi \quad (4)$$

where $f(\phi)d\phi$ is the probability that the fiber axis lies between ϕ and $\phi + d\phi$.

Basis Weight: The basis weight was measured as an average value based on five 100 cm² cutouts randomly distributed over the fabric width according to ASTM small swatch method [29].

Tensile Strength and Elongation: Typical tensile tests performed on nonwoven fabrics use rectangular “strip” samples that are usually 2.54 or 5.08 cm (1 or 2 inch) width [30]. Due to frequent specimen breaks at the clamp face during tensile strip testing, a modified tensile method was developed. A “dog bone” sample shape given by ASTM D 638-03 (type III) was used [31] to prevent breakage at the clamp. This shape is commonly used for standard testing of tensile properties of plastics. The testing length of this “dog bone” specimen is 57 mm (2.25”) and in the narrow portion, the width is 19 mm (0.75”). A testing rate of 228 mm/min was used to maintain same strain rate as the ASTM strip test (400%/min)[30]. Tensile strengths are reported as normalized stress N/(g/m²)/2.5 cm) (lb/(g/m²)/inch).

Results And Discussion

Thermal Analysis: The first step in melt blowing is to melt the polymer. To understand the melting characteristics, DSC thermal scans were obtained. The endothermic ranges and endothermic peaks are shown in *Table 1*. Polymer 80A exhibited a distinct endothermic peak at 111.1°C and a small peak at about 160°C region. 90A had a smaller peak at 112°C and a more pronounced endothermic peak at 170.5°C, while 98A had a small peak shifted to 124.1°C and a major peak at 180.5°C. The lower temperature endothermic peaks have been attributed to the loss of hydrogen bonding between the NH-groups in the urethane linkage and the O-groups in the polyether segments. The higher temperature endothermic peaks are due to the hard-segment melting and disappearance of the hard-segment domains[32].

After melt blowing, the lower endothermic peak temperature decreased dramatically, by approximately 50°C, for 98A and by approximately 40°C for 90A and 80A. It is not clear why this happens. The upper endothermic peak temperature change was much less pronounced for 98A and 90A, only about 5°C. However, this endothermic peak for 80A disappeared. Since the higher temperature endothermic region is due to melting of the hard-segments and since high temperature processing of polyurethanes results in the dissociation of urethane linkages in the hard-segments[33] and thus the destruction of the hard-segments, the observed reduction in the amount of the high temperature endothermic peak and a small shift to lower temperatures is expected.

Table 1. TPU Properties and Melt Blowing Die Temperatures

Polymer	Die Temperature (°C)	Solution Viscosity			Endothermic Range		Local Maxima	
		Pellets (cP)	Webs (cP)	Ratio	Onset (°C)	End (°C)	T _{M1} (°C)	T _{M2} (°C)
80A	227	152	34 ± 7	0.22	87	177	111	160
90A	250	141	37 ± 1	0.26	80	187	112	171
98A	261	149	31 ± 1	0.21	87	212	124	181

Solution Viscosity: In melt blowing, it is preferred to have a polymer with a low melt viscosity. This can be achieved by using a low molecular weight polymer or by using high temperatures. In the current study, the temperature was used to control the pressure on the melt blowing die. BASF kindly provided the solution viscosity data of polymeric material obtained from both polymer pellets and melt blown materials. The viscosity data for the original pellets and for the polymer after web formation is shown in *Table 1*. In all cases, the solution viscosity of the polymer in the webs dropped to 21-26% of its original value in the pellets, i.e. $\eta_{\text{web}} \sim 0.21-0.26 * \eta_{\text{pellets}}$. It is well known that polyurethanes degrade at high temperatures due to a shift in the equilibrium between chain formation and chain dissociation. Hentschel and Munstedt[33] measured the loss of molecular weight in the temperature range 160-220°C for similar polyurethanes with the same hard segment. Using gel permeation chromatography (GPC), they found that the molecular weight decreased to 44% of its original value within 5 minutes at 220°C. Using their analysis, which assumed only thermal degradation and used only very low shear stresses, the molecular weight of the webs in our study should be 28-41% of the molecular weight of the original pellets. According to the Mark-Houwink-Sakarada equation for a good solvent, the solution viscosities of the webs should be 37-50% of the solution viscosities of the pellets (i.e. $\eta_{\text{film}} \sim 0.37-0.50 * \eta_{\text{pellets}}$). Hentschel and Munstedt also found that the polydispersity decreased at higher temperatures, which would reduce the solution viscosity further. Although we observed significantly larger decreases in the solution viscosities ($\eta_{\text{web}} \sim 0.21-0.26 * \eta_{\text{pellets}}$), we note that the residence time of the molten polymer in NCRC's melt blowing equipment is estimated to be 20 minutes and uses higher shear stresses. Thus the degradation of the polyurethanes used in this study should be more severe than that of Hentschel and Munstedt's study. The properties of the web reported throughout this article are those of the degraded polymer, not of the original material.

Fiber Diameter Distributions: Scanning electron microscopy images of each web were obtained. *Figure 1* shows a typical SEM of one of the melt blown webs. Fiber diameter distribution data were collected for all melt blown samples (*Figure 2*) from similar SEM images. The most probable fiber diameter is approximately 5 microns and virtually all fiber diameters are ≤ 20

microns. The distributions are nearly identical for all of the webs made in this study. This data is comparable with fiber diameter distributions obtained for melt blown fabrics made with more conventional polymers [34].

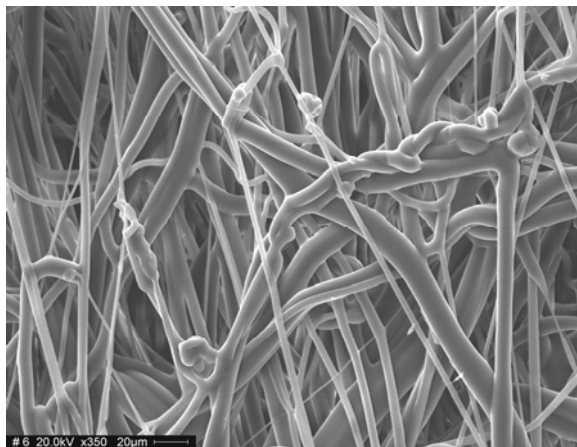


Figure 1. Structure of polyether based thermoplastic polyurethane melt blown substrate (Courtesy of BASF).

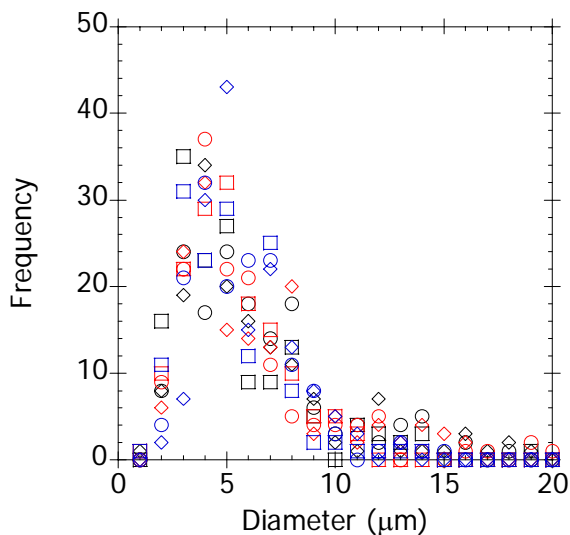


Figure 2. Fiber diameter distribution functions for melt blown webs. Black symbols are for webs made with polymer 80A, red symbols are made with polymer 90A and blue symbols are made with polymer 98A. Squares are for webs made at a DCD of 14 cm, diamonds for DCD = 20.3 cm, and circles for DCD = 30.5 cm.

Fiber Orientation Distribution Function (ODF) of Melt Blown Samples: The fiber orientation distribution function histograms were obtained for all samples made in this series. The cosine squared anisotropy ratio, H_t , varied from -0.038 to -0.14, indicating slightly higher frequency of fibers oriented in machine direction. H_t did not correlate with polymer type, die-to-collector distance or basis weight (collector belt speed). Thus, the fibers are slightly oriented in the machine direction as expected for melt blown webs.

Tensile Testing: As discussed previously, the tensile data could not be obtained with the conventional strip test, since all specimens broke at the grips. Thus a "dog bone" specimen was used. To convert the displacement of the grips to elongation of the narrow section of the dog bone specimen, a conversion equation was developed by graphing the distance between two marks on the narrow section of the dog bone vs. the testing machine displacement. A straight line with a slope of 1.17 was found to account for this difference for all polymer grades and for the range of displacements used in these experiments (data not shown). Thus, the elongation of the narrow tested area of the specimen was 1.17 times the instrumental elongation.

Fabric tensile strength and elongation in the machine and cross directions were obtained for all melt blown nonwoven samples. The tensile strength and elongation for several 90A polymer grade melt blown specimen at a DCD of 14 cm could not be measured because the instrument

crosshead reached the extension limit (400%) before the sample failed. The tensile strengths of the remainder of the specimens were normalized by dividing by the basis weight and the sample width, while the elongation was corrected for the dog bone shape. Tensile strength and elongation were plotted as a function of die-collector distance, DCD (*Figure 3*). It is obvious that melt blown fabrics made with 98A achieved higher tensile strength but lower elongation to failure than 80A. This is the expected behavior for similar polymers that differ primarily by their hardness. Machine direction tensile values were noticeably higher than those in cross direction, which is most likely associated with the slightly higher fiber orientation in machine direction that was measured on these samples.

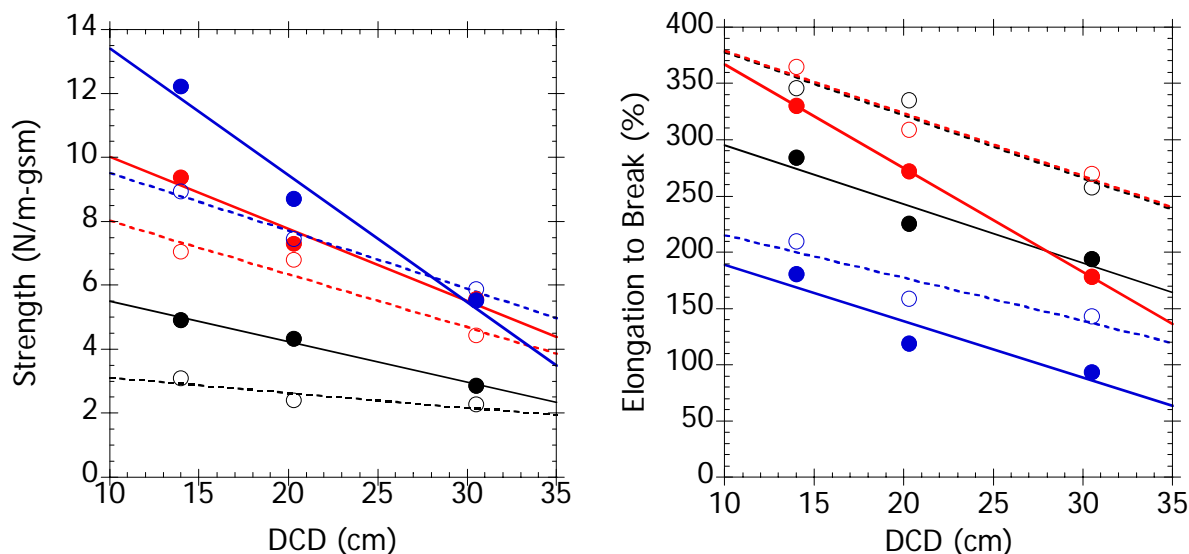


Figure 3. Tensile strengths (left) and elongation to break (right) of the webs are shown. Solid symbols are for the machine direction while open symbols represent the cross direction data. Solid lines are linear regressions of the machine direction data, while dashed lines are for the cross direction. Black symbols are for polymer 80A, red for polymer 90A, and blue for polymer 98A derived webs.

The tensile strength *and* the elongation both decreased with an increase of die to collector distance, both dropping 25-50% as DCD increased from 14 to 30.5 cm. Furthermore, the tensile strength decreased more rapidly with DCD for polymers with higher hardness. This behavior is quite different from what would normally be expected for elastomers. Usually, one would expect that, as the tensile strength decreased, the elongation to failure would increase. Indeed, Lee and Wadsworth [35] found for polypropylene melt-blown webs that, at low die temperatures, the tensile strength decreased with increasing DCD, but the elongation to break increased. At higher die temperatures, the tensile strength first increased then decreased as DCD increased. The elongation to break, however, always increased with DCD. Thus, our results for thermoplastic polyurethanes differ markedly from those of Lee and Wadsworth for polypropylene. To

understand the observed behavior, one must first understand the development of strength in a melt blown web.

In melt blowing, very little orientation of the polymer chains within the fibers is expected to occur, so there is no increase in fiber strength due to extension-induced molecular orientation. Furthermore, since there is no molecular orientation, the amount of crystallinity depends only on polymer type and the time allowed for the sample to cool. Since the fiber morphology is expected to be nearly the same for all webs within the same polymer species, the fiber strength depends only on the polymer properties, not on fiber morphology. Thus, each fiber within the web should have similar tensile strength and similar elongation to break. In other words, differences in the web strength and elongation for any one polymer type must depend on web properties, such as fiber orientation or inter-fiber bonding, and not on fiber properties. Since we saw similar fiber orientation patterns within all produced samples, the changes in web mechanical properties can be attributed primarily to fiber-to-fiber bonding.

During web formation in melt blown nonwovens, the newly created fibers travel from the die to the forming belt. The amount of time that it takes for the fibers to traverse this distance depends only on the DCD when the process air velocity is unchanged. During this time, the fibers begin to solidify. The extent to which they have solidified depends strongly on the time it takes for them to travel from the die to the collector. For short DCD, the fibers are still soft and sticky upon landing on the forming belt and upon other fibers forming the web. They do not solidify completely until after forming the web. Under these conditions, we would expect the fibers to be well adhered to each other and thus form a strong web. On the other hand, for long DCD the fibers have solidified to a much greater extent as they travel to the forming belt. Although they may complete their solidification on the forming belt, much less solidification occurs in the web. During this process, if too much solidification has occurred prior to web formation little or no adhesion develops between the fibers on the forming belt and the web has low strength. This is often observed as high loft melt blown nonwovens.

This is clearly seen in the present study. *Figure 4* shows load-displacement curves for three different DCDs for the 90A hardness polyurethane. Three specimens for each DCD are shown. (Similar curves are seen for 80A and 98A – not shown.) Note that the load-displacement curves are nearly identical for all specimen and all DCDs, with the exception of their elongation to break and tensile strength. The similarity of the load-displacement curves indicate that both the fiber morphologies and the web structures are nearly the same in all of the webs. As DCD increases, the point at which the web fails occurs at lower loads. Since the curves lie nearly on top of each other, this forces the elongation to break to also be shorter. This can be understood as follows. As one stretches a web made from these fibers, the stress increases until it reaches the strength of the interfiber adhesion. At this point, the fibers, and hence the web, separate; i.e. the web fails. As the interfiber adhesion decreases, this point is reached at lower and lower stress levels; hence the tensile strength of the web decreases. Likewise, as the adhesive strength decreases and the web is stretched, the point at which the stress reaches the adhesive strength between fibers is reached at lower and lower elongations (refer to *Figure 4*). Hence the elongation to break as well as the tensile strength decreases as the interfiber adhesion decreases and the interfiber adhesion decreases with increasing DCD because more solidification of the fibers occurs before the fibers reach the forming belt.

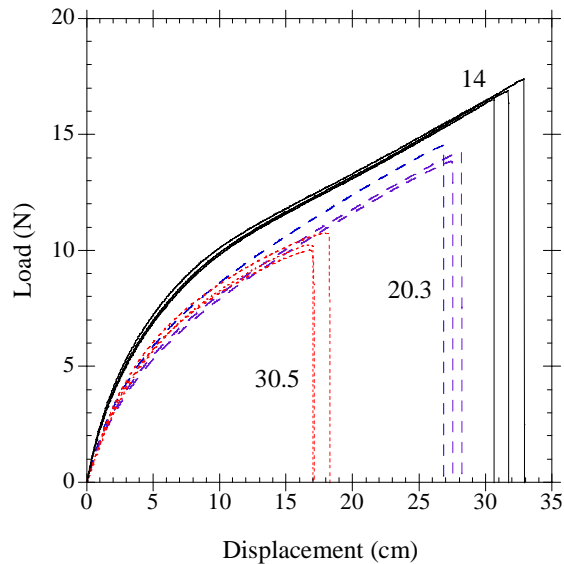


Figure 4. Load-displacement curves for 90A webs, three replicates for each DCD. Numbers on curves are the DCD.

Thus the tensile data reflect a combination of three effects: 1) the inherent elastomeric properties of each polymer grade, 2) the degree of inter-fiber bonding, which is influenced by the degree of solidification attained at collection point, and 3) the degree of alignment of fibers in the test direction, i.e. the ODF of the fibers.

Conclusions

A series of melt blown samples made with thermoplastic elastomers was produced and tested to investigate the nature of their structure-property relationship in melt blown process. The thermoplastic elastomer polymers used in this study were ether based polyurethanes with MDI-BDO hard segment structure. The three durometer hardness grades used were 80A, 90A and 98A. Solution viscosity measurements showed a decrease of 75-80% after spinning due to the high temperatures employed in the melt blowing nonwoven process. Differences in endothermic peak temperatures in polymer pellet and fabric samples were also observed.

Fiber diameter distributions measured on melt blown samples ranged from sub-micron to 20 microns with the most probable value at approximately 5 microns. These values are comparable in range with fiber diameter distributions measured on melt blown samples made with more conventional polymers such as polypropylene.

From mechanical property data it is apparent that several mechanisms are influencing tensile and elongation behavior including DCD, polymer hardness and fiber ODF of the samples related to the tested direction. It was shown that the main effect of increasing DCD is that longer DCDs

result in more time for solidification to occur before the fibers come into contact with each other on the forming belt. This results in reduced interfiber adhesion at long DCDs and thus lower tensile strengths and lower elongations to break.

Acknowledgements

The authors thank NCRC member companies for funding this project. Further, we express our appreciation to BASF Corporation and in particular to Dr. Toprak Serhatkulu, who provided polymer materials, SEM images, solution viscosity data and certain DSC data on pellet and fabric samples.

References

1. U.S. Pat. No. 6,784,127
2. U.S. Pat. No. 4,820,572
3. U.S. Pat. No. 4,803,117
4. U.S. Pat. No. 4,660,228
5. U.S. Pat. No. 4,908,263
6. U.S. Pat. No. 4,777,080
7. U.S. Pat. No. 5,324,580
8. U.S. Pat. No. 4,707,398
9. U.S. Pat. No. 4,813,948
10. U.S. Pat. No. 5,230,701
11. U.S. Pat. No. 4,741,949
12. Nonwovens Report International, 235 (1990)
13. Nonwovens Report International, 251 (1992)
14. Holden, G., Legge, N.R., Quirk, R.P., Schroeder, H.E.: Thermoplastic Elastomers, 2nd edition, Hanser Publishers, 1996
15. Holden, G.: Understanding Thermoplastic Elastomers, Hanser Publishers, 2000

16. Bonart, R., *Polymer* **20** (11) 1389-1403 (1979)
17. Cooper, S.L., Tobolsky, *J Appl. Polym. Sci.* **10** 1837 (1966)
18. Bonart R., Morbitzer, L., Hentze, G., *J Macromol. Sci.* **B3** 337 (1969)
19. Quay, J.R., Sun, Z, Blackwell, J, *Polymer* **31**(6) 1003-1008 (1990)
20. Nigar, M., Chvalun, S.N., Blackwell, J., *Acta Polymer* **49** 27-34 (1998)
21. Blackwell, J., Quay, J.R., Nagarjan, M.R., Born, L., Hespe, H., *J. Polym. Sci Part B Polym. Phys.* **22** (7) 1247-1259 (1984)
22. Blackwell, J., Lee, C.D., *J. Pol. Sci. Pol. Phys.* **22** (4) 759-772 (1984)
23. Blackwell, J., Nagarajan, M.R., *Polymer* **22** 202 (1981)
24. Blackwell, J., Nagarajan, M.R., Hoitink, T.B., *ACS Symp. Ser.* 172-179 (1981)
25. ASTM D2240-00
26. Wentz, V.A., *Ind. and Eng. Chem.* **48** (8) 1342-1346 (1956)
27. Pourdeyhimi, B, Dent, R, *Textile Research Journal* **69** (4) 233-236 (1999)
28. Jeddi A.A.; Kim H.S.; Pourdeyhimi B., *International Nonwovens Journal*, Vol. **10**(3) 10 (2001)
29. ASTM D 3776
30. ASTM D 5035-95
31. ASTM D 638-03
32. Wirpsza, Z.: *Polyurethanes Chemistry, Technology and Applications*, Ellis Horwood, New York, 1993.
33. Hentschel, T., Munstedt, H., *Polymer* **42** 3125-3202 (2001)
34. Culloch, J.G., *International Nonwovens Journal* **8**(1) 66-72 (1999)
35. Lee, Y., Wadsworth, L. C., *Polymer* **33**(6) 1200-1209 (1992)